Journal of Cellular Physiology

Nitric Oxide Up-Regulates RUNX2 in LNCaP Prostate Tumours: Implications for Tumour Growth In Vitro and In Vivo

HEATHER NESBITT,[1]* GILLIAN BROWNE,[2] KATIE M. O'DONOVAN,[1] NIALL M. BYRNE,[3] JENNY WORTHINGTON,[1,4] STEPHANIE R. MCKEOWN,[1] AND DECLAN J. MCKENNA[1]

[1]*Biomedical Science Research Institute, University of Ulster, Coleraine, Londonderry, Northern Ireland*

[2]*Department of Biochemistry and Vermont Cancer Center, University of Vermont College of Medicine, Burlington, Vermont*

[3]*Bone Biology Division, Garvan Institute of Medical Research, Darlinghurst, Sydney, Australia*

[4]*Axis Bioservices Ltd., Research Laboratory, Coleraine, Londonderry, Northern Ireland*

Aberrant expression of the transcription factor RUNX2 in prostate cancer has a number of important consequences including increased resistance to apoptosis, invasion and metastasis to bone. We previously demonstrated that hypoxia up-regulated RUNX2 in tumour cells, which in turn up-regulated the anti-apoptotic factor Bcl-2. Here, we investigate the impact of nitric oxide (NO) on RUNX2 and Bcl-2 expression in prostate cancer and further, how RUNX2 over-expression can impact tumour growth, angiogenesis and oxygenation in vivo. The effect of NO levels on RUNX2 and thus Bcl-2 expression was examined in prostate cancer cells in vitro using methods including gene and protein expression analyses, nitrite quantitation, protein-DNA interaction assays (ChIP) and viability assays (XTT). The effect of RUNX2 over-expression on tumour physiology (growth, oxygenation and angiogenesis) was also assessed in vivo using LNCaP xenografts. A low (but not high) concentration of NO (10 μM) induced expression of RUNX2 and Bcl-2, conferring resistance to docetaxel. These effects were induced via the ERK and PI3K pathways and were dependent on intact AP-1 binding sites in the RUNX2 promoter. RUNX2 over-expression in LNCaP tumours in vivo decreased the time to tumour presentation and increased tumour growth. Moreover, these tumours exhibited improved tumour angiogenesis and oxygenation. Low levels of NO increase expression of RUNX2 and Bcl-2 in LNCaP prostate tumour cells, and in vivo up-regulation of RUNX2 created tumours with a more malignant phenotype. Collectively, our data reveals the importance of NO-regulation of key factors in prostate cancer disease progression.

J. Cell. Physiol. 231: 473–482, 2016.

Recent statistics show that approximately 40,000 men are diagnosed with prostate cancer annually in the UK (Mayor, 2012). Although early stage prostate cancer can be successfully treated with androgen-dependent therapy, patients often relapse and develop more aggressive, metastatic disease. Many aspects of the tumour microenvironment, including hypoxia, pH and nitric oxide (NO) levels, contribute to malignant progression of tumours (Frederiksen et al., 2007; Webb et al., 2011; Browne et al., 2012). A fundamental challenge in improving prostate cancer treatment is to understand which molecular pathways and genes are affected by these microenvironmental factors in the promotion of malignant progression.

RUNX2 is an osteogenic transcription factor which normally maintains a balance between bone formation and resorption by regulating expression of various genes (Komori, 2003). Its expression is significantly up-regulated in prostate (Akech et al., 2010), breast (Pratap et al., 2008; Shore et al., 2005) and colon cancer (Wai et al., 2006). Aberrant RUNX2 expression has been shown to contribute to a more aggressive, metastatic phenotype by altering expression of many genes involved in migration, invasion, metastasis, apoptosis and angiogenesis (Ho et al., 2009; Akech et al., 2010; Browne et al., 2010). Recently, we demonstrated that hypoxia induced RUNX2 expression in cancer cells, resulting in increased expression of the anti-apoptotic gene Bcl-2 (Browne et al., 2012). However, it is likely that other factors in the tumour microenvironment also impact upon RUNX2 levels. There is some evidence to suggest that NO is capable of regulating RUNX2 expression in osteoblasts (Damoulis et al., 2007; Sheu et al., 2012), but no study to date has investigated if RUNX2 expression is similarly influenced by NO levels in prostate cancer.

NO is a soluble gas produced by nitric oxide synthases (NOS), of which there are three isoforms. Inducible NOS (iNOS) generates micromolar levels of NO, whereas endothelial NOS (eNOS) and neuronal NOS (nNOS) produce nanomolar concentrations. The control of NO flux exerted by this trio of synthases has important functions in tumour growth, apoptosis and angiogenesis, with both pro- and anti-tumour effects observed; low levels of NO encourage cell proliferation, whereas high concentrations inhibit growth (Burke et al., 2013). In prostate cancer, increased expression of iNOS and eNOS has been positively correlated with advanced tumour progression (Cronauer et al., 2007; Nanni et al., 2009). However, these observations do not necessarily reflect the relative concentrations of NO present in the tumours, nor do they identify all the molecular pathways affected by NO which may contribute to prostate cancer progression.

Completing Interests: There are no completing interests.

*Correspondence to: Heather Nesbitt, Biomedical Science Research Institute, University of Ulster, Coleraine, Northern Ireland, UK BT44 8DZ. E-mail: h.nesbitt@ulster.ac.uk

Manuscript Received: 7 July 2015
Manuscript Accepted: 16 July 2015

Accepted manuscript online in Wiley Online Library (wileyonlinelibrary.com): 19 July 2015.
DOI: 10.1002/jcp.25093

Clearly, more focused studies are required to unravel the complex role of NO in the progression of this disease. To this end, we examined the contribution of NO in the regulation of RUNX2 expression in prostate cancer. Furthermore, we investigated the impact of RUNX2 over-expression on the anti-apoptotic protein Bcl-2 and the subsequent effects on tumour growth and malignant progression.

Materials and Methods

Cell culture

The prostate adenocarcinoma cell line, LNCaP was maintained in RPMI-1640 media, containing L-glutamine, 10% foetal bovine serum (FBS). LNCaP cells stably transfected with vectors containing wild-type RUNX2 (LNCaP-R) or empty vector (LNCaP-C) were generated previously (Browne et al., 2012); these cells were maintained under the same conditions as the parental LNCaP cells. PC3 cells were maintained in RPMI-1640 media containing 10% FBS. MCF-7 breast cancer adenocarcinoma cells were grown in DMEM medium containing L-glutamine (580 mg/L), D-glucose (1 g/L), sodium pyruvate (110 mg/L), 10% FBS and 1% penicillin. All cells were obtained from ATCC, Rockville, MD, USA and were cultured at 37°C under 5% CO_2 in air.

Drug preparation

All drugs were obtained from Sigma, Gillingham, UK unless otherwise stated. Stock solutions of the following drugs were prepared in PBS: NOC-18 (NO-donor, 100 μM; Calbiochem, Tokyo, Japan), haemoglobin (NO scavenger, 50 μM) and actinomycin D (500 μM). Drugs were dissolved in DMSO and diluted appropriately following manufacturer's instructions: U0126 (MEK inhibitor;10 mM), wortmannin (PI3K/AKT inhibitor; 2 mM), Src Inhibitor 1 (10 mM), SP600125 (JNK inhibitor;20 mM), SB202190 (10 mM), docetaxel (anti-mitotic chemotherapy; 20 mM stock) and bicalutamide (non-steroidal antiandrogen) (Santa Cruz Biotechnology, Heidelberg, Germany).

Gene expression analysis

RNA was extracted using Trizol® (Invitrogen, Paisley, UK) and reverse transcribed using RevertAid reagents according to manufacturer's instructions (Fermentas, Cambridge, UK). Real-Time Quantitative PCR (RT-Q-PCR) was carried out using SYBR green (Fermentas, Cambridge, UK) and gene specific primers (Supplementary Table 1) in a Lightcycler 480 (Roche, Welwyn Garden City, UK). After normalization to the reference gene (as indicated), relative expression levels of each target gene were calculated using the comparative C_T (ΔΔCT) method. Data were obtained from three independent experiments performed in triplicate.

Western blotting

Protein was extracted using RIPA buffer (Pierce, Rockford, UK). Primary antibodies used were RUNX2 (57K) (1:750), Bcl-2 (DC-21) (1:500) and β-actin (H-300) (1:1,000). Membranes were blocked in 5% BSA diluted in 1× TBS-T (0.05%) followed by incubation in the appropriate secondary antibody [goat anti-rabbit IgG-HRP (1:10,000) or goat anti-mouse IgG-HRP (1:10,000)]. All antibodies were purchased from Santa Cruz Biotechnology, Heidelberg, Germany.

Nitrite quantitation assay

Following eNOS transfection, NO released by NOC-18 was analysed using a NO Quantitation Kit (Active Motif, La Hulpe, Belgium) according to manufacturer's instructions, alterations included growing LNCaP cells in RPMI. Absorbance was read at 540 nm using a FLUCOstar Omega microplate reader (BMG Labtech, Ortenberg, Germany).

RNA stability assay

LNCaP cells were treated with NOC-18 (10 μM) at a final concentration of 10 μM. After 8 h, cells were treated with actinomycin D at a final concentration of 5 μM. RNA was extracted for subsequent gene expression analyses 0, 4, 6 and 8 h after treatment.

Plasmid DNA isolation

Plasmids (Supplementary Table 2) containing the complete RUNX2 promoter region, RUNX2 promoter deletion constructs (Drissi et al., 2000) or eNOS constructs (Gene Copoeia, Rockville, MD and Supplementary Fig. 6) were transformed using DH5α competent cells according to manufacturer's instructions (Invitrogen, Paisley, UK). Subsequently, plasmids were purified using Purelink HiPure Plasmid DNA purification kit according to manufacturer's instructions (Invitrogen, Paisley, UK).

Transient DNA transfection

LNCaP cells were transfected with the various plasmids using Fugene HD (Roche, Welwyn Garden City, UK) according to manufacturer's instructions. Transcriptional activity of the RUNX2 promoter in the presence of NO (10 μM) was measured via a Dual-Glo Luciferase Assay System according to manufacturer's instructions (Promega, Southampton, UK).

siRNA transfection

LNCaP cells were transfected with smart pool RUNX2 siRNA (100 nM; Thermo Fisher Scientific Biosciences, Opelstrasse, Germany) using siRNA DharmaFECT 2 regent (Thermo Fisher Scientific Biosciences). Control non-targeting siRNA-A (100 nM; Santa Cruz Biotechnology, Heidelberg, Germany) was used as a negative control. RUNX2 knockdown was confirmed via RT-Q-PCR and western blotting.

Chromatin immunoprecipitation (ChIP) assay

A ChIP IT Express Enzymatic Assay (Active Motif, La Hulpe, Belgium) was used to measure RUNX2 interaction with proposed binding sites within the Bcl-2 promoter (Supplementary Fig. 7) in the presence of NO. LNCaP cells were treated with NOC-18 treated (10 μM) for 24 h. PC3 cells were used as a positive control for RUNX2 expression (Akech et al., 2010).

Cell proliferation XTT assay

LNCaP cells were seeded, transfected with control or RUNX2 siRNA, and treated with NOC-18 (10 μM) for 16 h. The cells were then treated with docetaxel (2 nM) for 48 h. LNCaP cells were seeded, treated with L-NAME (0.1 mM) in combination with docetaxel (10 nM) for 48 h. An XTT assay (Roche, Welwyn Garden City, UK) was carried out to measure cell viability. Absorbance was measured at 492 nm using a FLUCOstar Omega microplate reader (BMG Labtech, Ortenberg, Germany).

All animal experiments were granted ethical approval by Home Office. Experiments were in accordance with the Animal Scientific Procedures Act 1986 and the UKCCCR guidelines for the welfare of animals in experimental neoplasia (Workman et al., 2010).

Tumour implantation

1×10^6 LNCaP-C (empty vector control) or LNCaP-R cells (RUNX2 overexpressing) (Supplementary Fig. 4) were re-

suspended in 100 μl of Matrigel (BD Bioscience, San Jose, CA) and implanted into the rear dorsum of Balb/c SCID mice (8–12 weeks old). Once tumours were palpable, calipers were used to measure tumour size according to the geometric mean diameter (GMD). GMD $= \sqrt[3]{\text{length} \times \text{breadth} \times \text{height}}$. Tumour doubling time was calculated by: selecting two tumour volume values within the exponential growth phase (e.g., 200 mm^3 and 400 mm^3 tumour volume), calculating time required to reach such volume and subtracting from the highest value.

Tumour oxygenation measurement

The oxygen partial pressure (pO_2) of tumours was recorded using an Oxylite oxygen electrode sensor (Oxford Optronics, Oxford, UK). Animals were secured into a bespoke restraining device with their tumours exposed. A fibre optic probe was inserted into a 21 gauge needle before subsequent insertion into the tumour tissue. The needle was withdrawn and the probe was left to stabilise for 10 min before readings commenced. Thereafter pO_2 values were recorded every 15 sec for 10 min. Readings were taken in three sites for each time point and all the results averaged.

Dorsal skin flap model

The specially designed window chamber (APJ Trading Co. Ltd., Ventura, CA) contains a viewing port into which tumour fragments or cells can be implanted on the exposed panniculus carnosus muscle. This chamber was sutured onto the dorsal area of male SCID mice, 3 days later the tumour cells (LNCaP-C or LNCaP-R) were implanted in the window chamber (1×10^5 per mouse) and subsequently grown for 10 days. To image the blood vessels, 150-kDa Fluorescein-Isothiocyanate (FITC) labelled dextran (50 μl of 50 mg/ml; Sigma) was injected into the tail vein using a 21 gauge needle. Within 15 min the mice were placed in a restraining equipment and images of the vasculature were taken with a confocal microscope (Leica, Solmes, Germany). Images were taken 2, 4, 6, 8 and 10 days after the implantation of cells.

Haematoxylin and eosin staining

At the end of the tumour growth assay, animals were sacrificed and lungs dissected and placed in 4% paraformaldehyde (PFA) (Sigma). The lungs were wax embedded and 5 μM sections were cut using a microtome (Leica, Phoenix, AZ). Sections were stained with haematoxylin and eosin (H & E) stained according to standard procedure (Sigma) mounted using DPX (Sigma) and cover slipped.

Immunohistochemistry

Tumours at the experimental endpoint were excised, fixed in PFA and wax-embedded. 5 μM sections were stained with RUNX2, Bcl-2 and IgG antibodies using Superpicture 3rd Gen IHC kit (Invitrogen, Paisley, UK). Immunohistochemistry staining was scored using a two approach method for extent and intensity (Braconi et al., 2008). Extent of staining was defined as the percentage of cells with nuclear (RUNX2) or cytoplasmic (Bcl-2) immunoreactivity and was scored 0–5: negative (0); $\leq$10% (1); 11–25% (2); 26–50% (3); 51–75% (4) and $\geq$76% (5). Intensity of staining was scored 0–3: negative (0); weak (1); moderate (2); strong (3). Scores were averaged with three mice per group.

Ethics

No human samples were required in completing data for this paper.

Results

NO concentration is critical for the induction of RUNX2

To investigate how different concentrations of NO affect RUNX2 expression, we used two methods to generate physiologically relevasnt levels of NO: (i) a slow-releasing NO donor (NOC-18) and (ii) transfection of the eNOS gene. The use of the NOC-18 donor gives insight into pathways regulated via NO, whereas the use of an eNOS-containing vector mimics eNOS transcription within a cancer cell and the resultant effect on RUNX2 expression. We carried out NO quantitation for both assays, demonstrating that the NOC-18 treated cells released more NO (~10 μM) compared to untreated (Fig. 1A). Similarly, in eNOS transfected cancer cells we determined that NO concentrations of ~10 μM and ~60 μM were released compared to untransfected after 24 and 48 h, respectively (Fig. 1B). We then investigated levels of RUNX2 mRNA and protein following treatment with various doses of drug or transfection over time. Figure 1C reveals that NO concentration is critical in determining RUNX2 mRNA expression: relatively low micromolar levels (10 μM) caused a significant increase, whilst higher levels (60–100 μM) caused a significant decrease. A similar trend is found when NO is generated by eNOS transfection: at 24 h (equivalent to a concentration of ~10 μM NO), RUNX2 expression was increased, whereas at 48 h (equivalent to a concentration of ~60 μM NO) RUNX2 expression was reduced compared to 24-h transfection (Fig. 1D). Thus, both methods of NO release demonstrate that the concentration of NO is critical in determining levels of RUNX2, with low micromolar levels increasing expression and high NO levels inhibiting the expression of RUNX2. The inhibition of NOS using L-NAME resulted in an increased sensitively against docetaxel treatment compared to docetaxel only (Fig. 1E). Furthermore, Fig. 1F reveals that L-NAME treatment resulted in a decrease in eNOS mRNA and consequently a reduction in RUNX2 and Bcl-2.

Low concentrations of NO Increase RUNX2 expression

Given the sharp increase in RUNX2 at low micromolar levels of NO (Fig. 1C), we further probed the effect of this exposure on prostate (LNCaP) (Fig. 2) and breast (MCF7) cancer cell lines (Supplementary Fig. 1), both known to express low levels of endogenous RUNX2 (Akech et al., 2010). In LNCaP cells, 10 μM NOC-18 treatment significantly increased expression of RUNX2 at both the mRNA (Fig. 2A) and protein level (Fig. 2B). To confirm that this induction of RUNX2 was due to NO levels, haemoglobin (a known NO scavenger) was used to inhibit NO effect. In the presence of haemoglobin, the induction of RUNX2 mRNA expression by NO was not observed (Fig. 2C).

Mechanisms of NO-mediated induction of RUNX2

To investigate why RUNX2 mRNA levels remained consistently elevated after treatment with NOC-18 (10 μM), we assayed the stability of RUNX2 mRNA levels under the same conditions. There was a significant difference in RUNX2 expression between NOC-18 treated cells and untreated controls 4, 6 and 8 h after actinomycin D treatment suggesting that NO helps stabilise RUNX2 mRNA (Fig. 3A). Previous studies have suggested that NO has the ability to activate or inhibit AP-1 (Haby et al., 1994; Tabuchi et al., 1996), which is relevant because there are two recognised AP-1 binding sites within the RUNX2 promoter (Rutberg et al., 1999) (Fig. 3B). Thus, to investigate how NO impacts RUNX2 expression, we used a series of RUNX2 deletion constructs in which the RUNX2 promoter had its AP-1 binding sites removed (Rutberg et al., 1999) (Supplementary Fig. 5). In LNCaP cells containing the intact

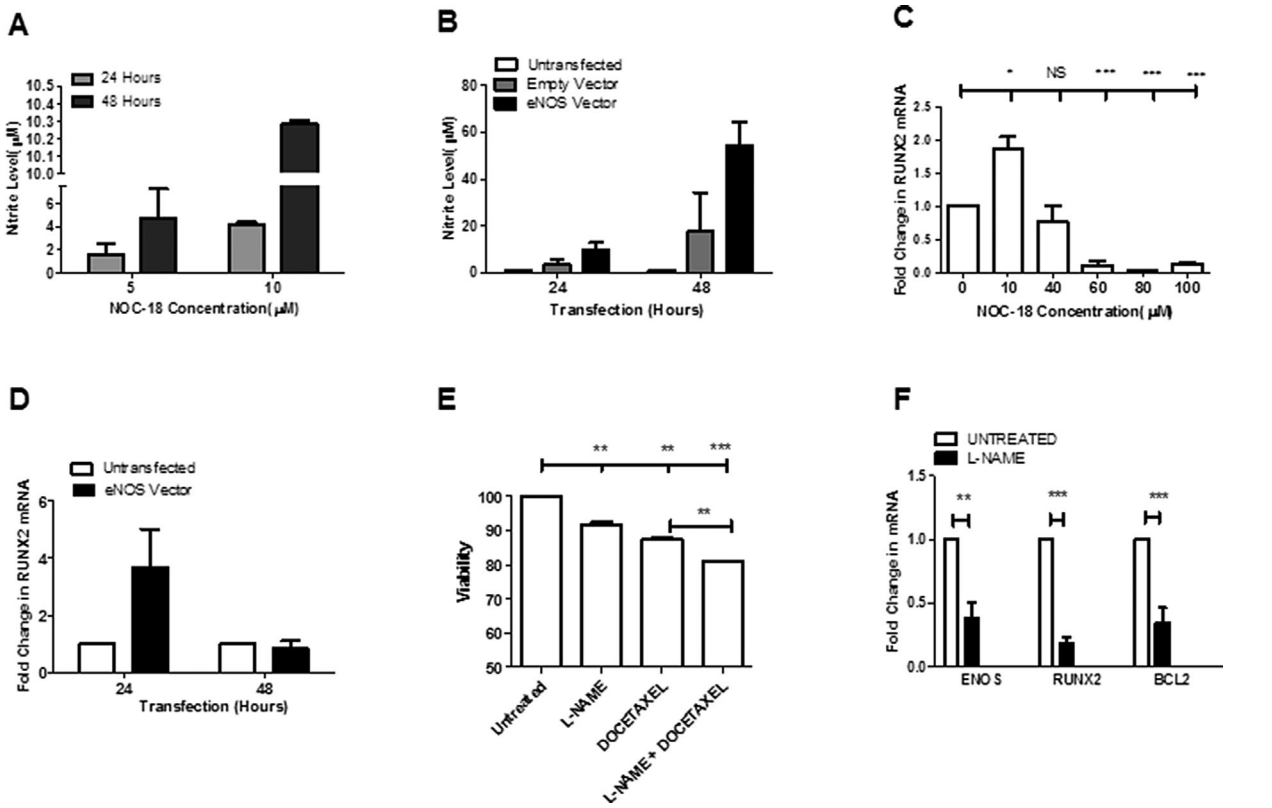

Fig. 1. NO concentration is a critical determinant of RUNX2 expression in LNCaP prostate tumour cells. (A) Nitrite levels in media from LNCaP cells when treated for up to 48 h with either NOC-18 (5 or 10 μM) or (B) transfection with eNOS or empty vector. (C) Fold change in RUNX2 mRNA relative to the reference gene hypoxanthine phosphoribosyl transferase (HPRT) in LNCaP cells following treatment for 48 h with NOC-18 (0–100 μM) (D) Fold change in RUNX2 mRNA relative to the reference gene HPRT in LNCaP cells following transfection with a vector containing the eNOS gene. (E) LNCaP cell viability in response to treatment with eNOS inhibitor L-NAME (0.1 mM) and/or docetaxel (2 nM). (F) Fold change in eNOS, RUNX2 and Bcl-2 mRNA levels following treatment with L-NAME. Results for all graphs are mean ± S.E.M of three independent experiments (n = 3). $^{*}P \leq 0.05$, $^{**}P \leq 0.01$, $^{***}P \leq 0.001$ (Students *t*-test). NS = not significantly significant.

RUNX2 reporter construct, NOC-18 (10 μM) increases transcription by approximately 2-fold (Fig. 3B). However, this induction was lost in cells transfected with the deletion constructs, in which one or both of the AP-1 site containing regions (p228-p490 and p490-p600) were absent from the RUNX2 promoter (Fig. 3B). A third mechanism of NO control RUNX2 expression was also tested, based on previous work which demonstrated that NO controls gene expression via protein kinase signalling (Pfeilschifter et al., 2001; Sparkmann and Boggaram, 2004). This involved examining the effect of a panel of inhibitors which target key signalling pathways, including JNK pathway (SP600125 inhibitor), P38 (SBS202190), ERK (U0126), P13K (Wortmannin) and SRC (SRC Inhibitor-1) to analyse RUNX2 levels (Sparkmann and Boggaram, 2004). In LNCaP cells untreated with NO, all inhibitors resulted in a down-regulation of RUNX2 at the mRNA level (Fig. 3C). However, only the inhibitors U0126 (ERK pathway) and Wortmannin (PI3K pathway) significantly inhibited the up-regulation of RUNX2 expression in the presence of NO, therefore implicating both the ERK and P13K pathways in the NO-mediated regulation of RUNX2 (Fig. 3D).

Effect of NO-mediated RUNX2 expression on downstream target genes

RUNX2 knockdown experiments confirm the knockdown in several downstream targets, including Bcl-2, VEGF and IL-8 (Akech et al., 2010). Furthermore, all three genes at an mRNA level are enhanced when treated with NOC-18 and inhibited in the presence of RUNX2 siRNA (Fig. 4A and B). Previously, we demonstrated that hypoxia-induced up-regulation of RUNX2 caused downstream up-regulation of Bcl-2 (Browne et al., 2012). We therefore investigated if NO-mediated levels of RUNX2 similarly impacted upon Bcl-2 expression. When LNCaP cells were exposed to NOC-18 (10 μM) the induction of RUNX2 was accompanied by a significant increase in Bcl-2 as measured both as mRNA (Fig. 4B) and protein (Fig. 4C) expression. Additionally, RUNX2 and Bcl-2 was significantly inhibited when cells were pre-treated with siRNA directed against RUNX2 (Fig. 4A–C).

To further confirm that RUNX2 was responsible for regulating Bcl-2 levels, we used LNCaP cells which over-expressed RUNX2 (LNCaP-R) compared to empty vector control cells (LNCaP-C) (Browne et al., 2012). LNCaP-R cells exhibited higher levels of RUNX2 and Bcl-2 than controls (LNCAP-C) (Fig. 4D). When LNCaP-R cells were transfected with siRNA directed against RUNX2, the reduction of RUNX2 levels resulted in a total loss of Bcl-2 protein expression within the cells (Fig. 4D). A ChIP assay was carried out to ascertain if this regulation was due to RUNX2 binding in the Bcl-2 promoter region (Fig. 4E). The assay revealed that NO exposure significantly increased the RUNX2 occupancy of both binding sites within the Bcl-2 promoter by 11% and 12%, respectively (Fig. 4E).

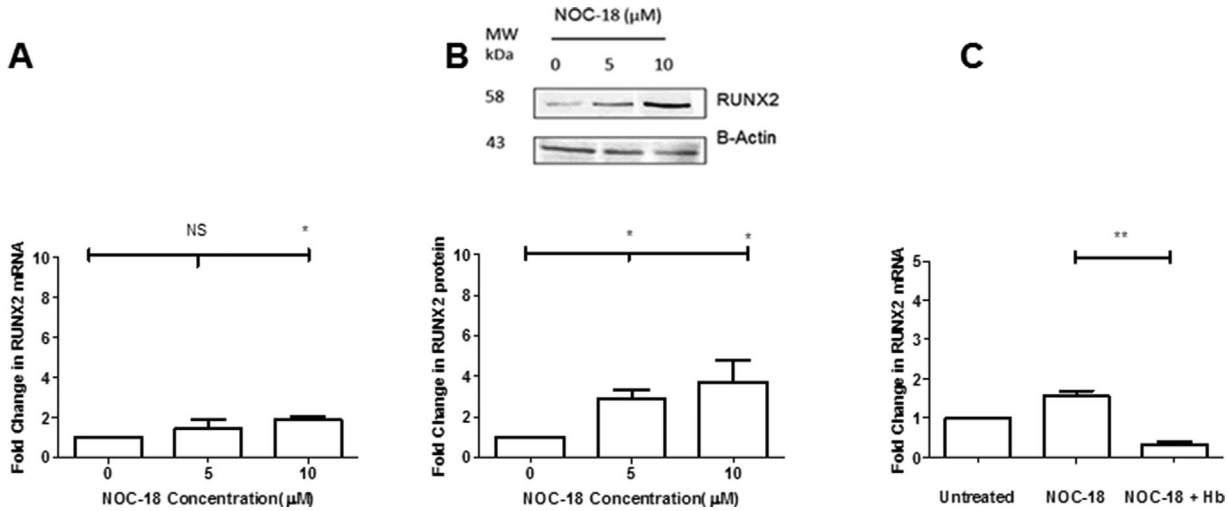

Fig. 2. NO concentration is critical for the induction of RUNX2 in LNCaP and MCF-7 cells. LNCaP cells were treated with NOC-18 (5 or 10 μM) or NOC-18 + inhibitor (Hb) and incubated for 48 h. Graphs show (A) RUNX2 mRNA fold change, relative to HPRT and (B) RUNX2 protein fold change, relative to β-actin, (C) RUNX2 mRNA expression after 48 h treatment with vehicle, NOC-18 (10 μM), or NOC-18 (10 μM) and haemoglobin (20 μM) in LNCaP. All data are displayed as mean ± S.E.M of three independent experiments performed in triplicate. $^{*}P \leq 0.05$, $^{**}P \leq 0.01$ (Students *t*-test).

We then wanted to see if this NO-mediated induction of both RUNX2 and Bcl-2 would impact upon cell viability. An XTT assay was carried out to investigate the effect of docetaxel in the context of these NO-mediated changes. LNCaP cells were transfected with control or RUNX2 siRNA, pre-treated with NOC-18 (10 μM) for 16 h and then exposed to docetaxel for 48 h. Figure 4F reveals viability was greater in cells pre-treated with NOC-18 in response to docetaxel compared to docetaxel treated only. Furthermore, knocking down RUNX2 via RUNX2 siRNA in NOC-18 and docetaxel treated cells showed a significant reduction in cell viability compared to control siRNA. NOC-18-treated cells, which were transfected with scrambled non-targeting siRNA, displayed a similar EC_{50} value for docetaxel to that obtained from cells which were treated with NOC-18 alone (7.4 nM compared to 8.2 nM) (Supplementary Table 3). However, in NOC-18-treated cells that were transfected with siRNA targeted against RUNX2, the EC_{50} value for docetaxel decreased to that exhibited by untreated cells (3.1 nM compared to 2.5 nM) (Supplementary Table 3). This confirmed that, when RUNX2 is inhibited, NO has no significant effect on cell viability.

Effect of RUNX2 over-expression in an LNCaP xenograft mouse model of prostate cancer

Since RUNX2 has been shown to drive expression of genes implicated in malignant progression (Akech et al., 2010; Browne et al., 2012), the LNCaP-R cells were implanted into mice to investigate the effect of RUNX2 on tumour physiology. Tumours arising from LNCaP-R cell implants grew more quickly, with palpable tumours arising within 60 days as compared with 86 days for LNCaP-C derived tumours (Fig. 5A). Furthermore, all mice implanted with LNCaP-R cells developed tumours (5/5 mice), compared to approximately 70% (5/7 mice implanted) for LNCaP-C. In addition, the LNCaP-R tumours had a faster doubling time (9.79 days) than LNCaP-C tumours (11.1 days), a difference that was evident by day 4 (Fig. 5B). Immunohistochemical analysis of tumours excised at the experimental endpoint confirmed that both Bcl-2 and RUNX2 were significantly up-regulated in the LNCaP-R tumours grown in vivo compared to controls (Fig. 5C). Analysis of lungs from these mice revealed a higher lung metastasis incidence % in animals bearing LNCaP-R (3/3 animals) tumours compared to LNCaP-C (1/3 animals) (Fig. 5D). Previously, it has been shown that RUNX2 can drive expression of angiogenesis-associated genes including VEGF (Browne et al., 2012). The dorsal skin flap model (Ming et al., 2013) was used to investigate the effect of over-expression of RUNX2 on the tumour vasculature. Imaging of the vascular pattern associated with LNCaP-R implants showed a more evenly distributed network of much smaller vessels with more branch points compared to that observed with control tumours (Fig. 6A–C). Given the distinct difference in these vascular patterns, we also measured tumour oxygenation during growth of subcutaneous tumours. These showed the tumours to be well oxygenated with a mean oxygen level of (23 mmHg (3.03%O_2) compared to control LNCaP-C tumours (5.85 mmHg (0.77%O_2) (Fig. 6D).

Discussion

Studies have shown that RUNX2 plays a role in the progression of prostate and breast tumour cells to a more aggressive and metastatic phenotype (Butterworth et al., 2008; Pratap et al., 2009). In this study, we investigated how various aspects of the prostate tumour microenvironment might influence the expression of RUNX2 and hence drive malignant progression. Previously, we have demonstrated that hypoxia induces up-regulation of RUNX2 expression, which in turn up-regulated Bcl-2 expression, thereby increasing resistance to apoptosis (Browne et al., 2012). However, we also suspected that NO levels within the tumour microenvironment would similarly impact upon RUNX2 expression, since RUNX2 is regulated by NO in osteoblasts (Damoulis et al., 2007; Sheu et al., 2012). The role of NO in tumour growth is complex, having been reported to have both pro- and anti-tumour effects, depending on concentration and extent of exposure (Brune, 2003; Burke

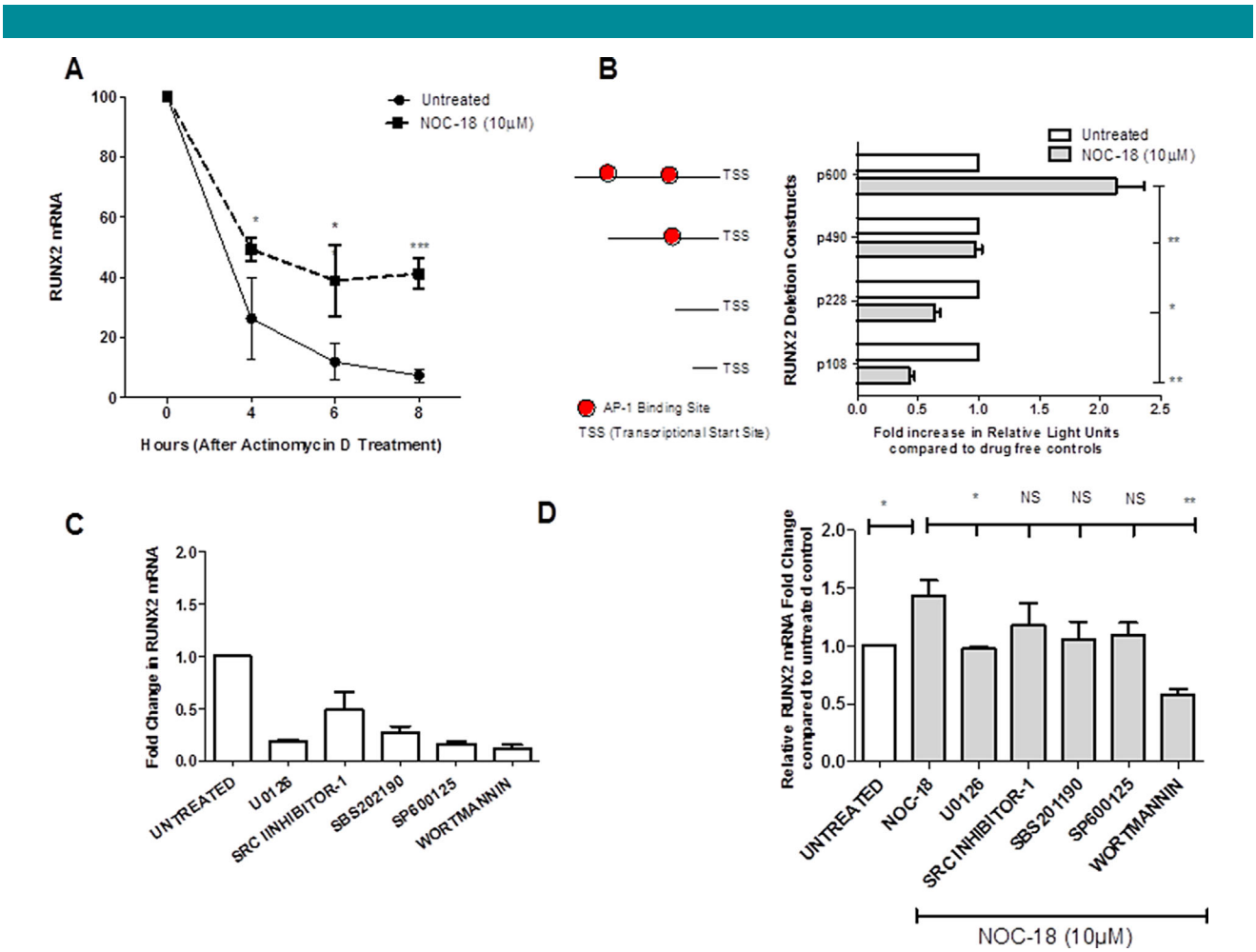

Fig. 3. Mechanisms of NO-mediated induction of RUNX2. (A) RUNX2 mRNA expression in LNCaP cells (relative to HPRT) treated with NOC-18 (10 μM) for 8 h, followed by treatment with actinomycin D (5 μM) for 0–8 h. (B) Luciferase assay carried out on LNCaP cells transfected with a variety of constructs before treatment with NOC-18 (10 μM) for 48 h. AP-1 binding sites within the RUNX2 promoter deletion constructs are depicted in the accompanying schematic. (C) RUNX2 mRNA levels in LNCaP cells treated with protein kinase inhibitors for 2 h in serum-starved media to maximise inhibition potential; U0126 (5 μM), Src Inhibitor-1 (10 μM), SBS202190 (10 μM), SP600125 (10 μM) and wortmannin (100 nM) for 48 h. HPRT was the reference gene. (D) The same treatments and analyses shown in (C) were carried out in the presence of NOC-18 (10 μM). All data are displayed as mean ± S.E.M of three independent experiments performed in triplicate. $^{*}P \leq 0.05$, $^{**}P \leq 0.01$, $^{***}P \leq 0.001$ (Students *t*-test).

et al., 2013). As a result, there is still conflicting evidence about the role and relevance of NO in prostate cancer progression. The current study proposed to shed light on this area by being the first to explore the relationship between NO and RUNX2 in prostate cancer cells.

We first demonstrated that NO concentration is critical in determining RUNX2 expression. Relatively low micromolar levels (10 μM) induced mRNA levels of RUNX2, whilst higher levels (≥ 60 μM) caused a decrease in LNCaP cells (Fig. 1C). This finding confirms the observations of many other studies demonstrating that NO can display dual and opposite functions, depending on its concentration (Burke et al., 2013). We were particularly interested in the effect of NO at levels of ≤10 μM, since this resulted in an increase in RUNX2, a transcription factor known to be associated with a more aggressive prostate cancer phenotype. We showed that these low levels of NO (≤10 μM) caused an increase in RUNX2 mRNA and protein expression in LNCaP cancer cells (Fig. 2A and B). We confirmed that these effects were indeed NO-mediated through the use of the NO scavenger haemoglobin (Fig. 1C). Our findings agree with previous work by Ho et al. (2009), who demonstrated that NO controls RUNX2 level in human osteosarcoma cells, which in turn causes an up-regulation in the anti-apoptotic protein Bcl-2.

We wanted to investigate possible mechanisms responsible for NO-mediated regulation of RUNX2. We first treated LNCaP cells with actinomycin D, a drug which inhibits transcription, to establish the effect of NO upon mRNA stabilisation. NOC-18 treatment (10 μM) resulted in a significant stabilisation of RUNX2 transcripts (Fig. 3A): this results in an increase in the length of time during which RUNX2 can activate target genes associated with cancer progression and is consistent with several previous report (Ho et al., 2009; Akech et al., 2010; Brown et al., 2012). This observation also corroborates previous studies that have shown that NO is responsible for stabilising several mRNA transcripts, including IL-8, p21 and TNF (Bakheet et al., 2003; Sparkman and Boggaram, 2004; Wang et al., 2008).

We investigated if NO influences RUNX2 transcriptional activity via increasing transcription factor binding within the

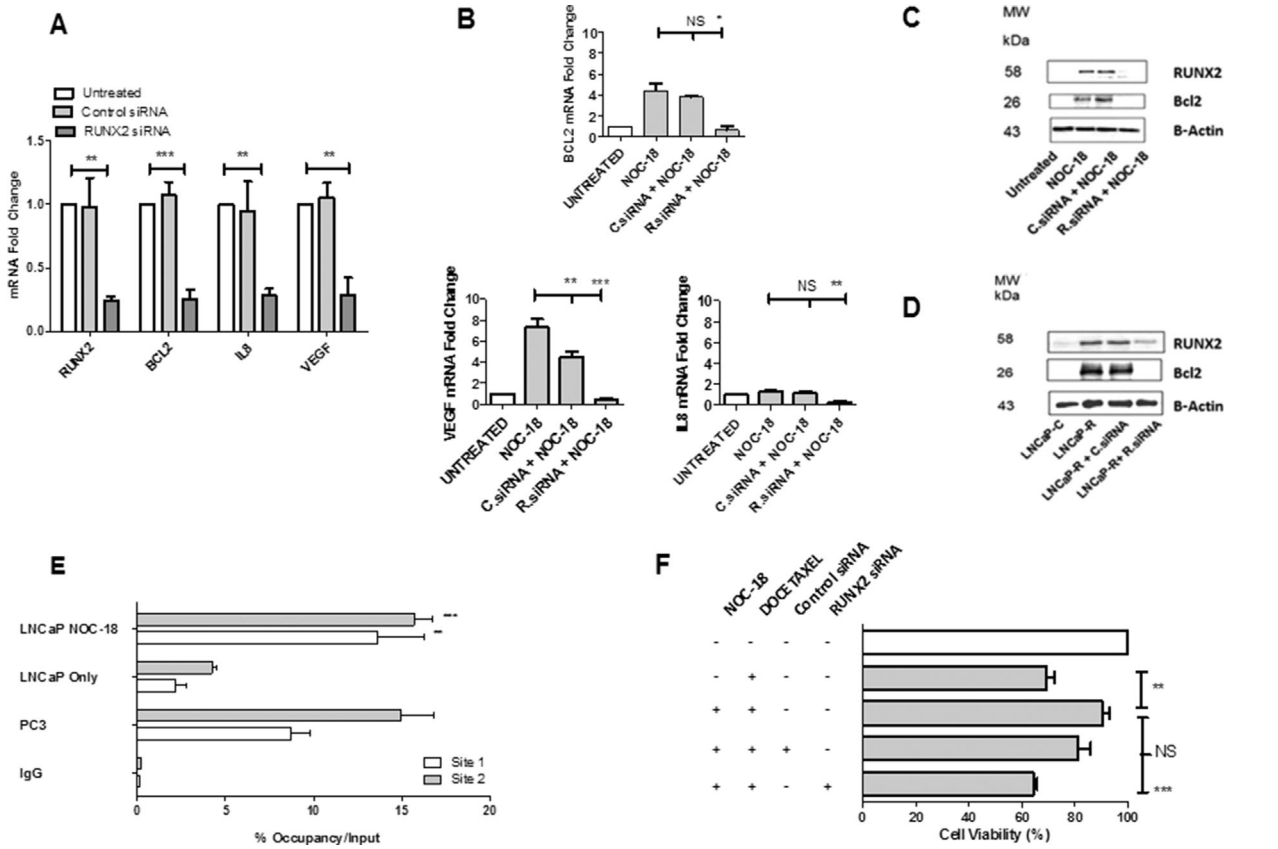

Fig. 4. NO-mediated RUNX2 expression impacts upon Bcl-2 levels. Fold mRNA change in RUNX2, Bcl-2, IL-8 and VEGF, relative to HPRT was examined in LNCaP cells were transfected with non-targeting control (C.siRNA) or RUNX2 siRNA (R.siRNA) for 24 h in the absence (A) or presence (B) of NOC-18 (10 μM) for 48 h. (C) Representative western blots show RUNX2 and Bcl-2 protein expression, with β-actin loading control. (D) LNCaP-C (Vector only) control cells and LNCaP-R (RUNX2 over-expressing) cells transfected with C.siRNA or R.siRNA for 48 h. Western blot shows RUNX2 and Bcl-2 protein expression, with β-actin loading control. (E) PC3 and LNCaP cells were untreated or treated with NOC-18 (10 μM) and incubated for 48 h. A ChIP assay was used to detect RUNX2 occupancy of two sites within the Bcl-2 promoter. IgG was used as a negative control and PC3 cells as a positive control. (F) LNCaP cells were transfected with C.siRNA or R.siRNA and treated with NOC-18 (10 μM) for 16 h. Following docetaxel treatment (2 nM) for 48 h, an XTT assay was carried out to measure cell viability. All data are displayed as mean ± S.E.M of three independent experiments performed in triplicate. $^{*}P \leq 0.05$, $^{**}P \leq 0.01$, $^{***}P \leq 0.001$ (Students *t*-test).

RUNX2 promoter. Given that AP-1 is a known NO regulated transcription factor (Jibiki et al., 2003) and has putative binding sites within the RUNX2 promoter (Rutberg et al., 1999), we speculated that AP-1 was involved in the transcriptional regulation of NO-mediated RUNX2 activity. By using constructs with deletions in the RUNX2 promoter, we confirmed that RUNX2 induction by NO was dependent upon the presence of intact AP-1 sites in the RUNX2 promoter (Fig. 3B). AP-1 is predominantly composed of protein dimers from the Jun and Fos families and both of these dimers have been reported as activating RUNX2 transcription (Wagner, 2002). Our results revealed that treatment of LNCaP cells with relatively low NO concentrations increased RUNX2 transcription due to increased AP-1 binding within the RUNX2 promoter.

It is known that NO diffuses across the cell membrane and interacts with the P13K, Src and the three MAPK (ERK, P38 and JNK) pathways, consequently altering gene expression (Pfeilschifter et al., 2001; Sparkmann and Boggaram, 2004). Therefore, we used a panel of pharmacological inhibitors to target these specific pathways in our cell systems (Fig. 3C and D). Inhibition of ERK (U0126) and P13K (wortmannin) significantly blocked the NO-mediated induction of RUNX2, suggesting this relationship is specifically dependent on these two pathways. This is in agreement with previous in vivo and in vitro studies in bone, which have revealed that both these pathways are involved in controlling RUNX2 (Xiao et al., 2002; Fujita et al., 2004; Ge et al., 2007).

A challenging aspect of prostate cancer treatment is to overcome chemoresistance, which is a key factor in the progression to advanced, metastatic disease. Ho et al. (2009) were the first to establish a link between NO, RUNX2 and Bcl-2, demonstrating that NO-mediated RUNX2 increased anti-apoptotic Bcl-2 in osteosarcoma MG63 cells. Since, we previously showed hypoxia conferred increased cell survival via RUNX2-mediated Bcl-2 expression (Browne et al., 2012), we wanted to see if NO levels increased cell survival in prostate cancer and whether this might also be important in chemoresistance. First, we confirmed that knockdown of RUNX2 resulted in knockdown of Bcl-2 in these cells, as well as other downstream targets such as VEGF and IL-8 (Fig. 4A). We then demonstrated that treatment of LNCaP cells with NOC-18 (10 μM) did indeed result in increased Bcl-2 expression (Fig. 4B). This effect was shown to be dependent on RUNX2,

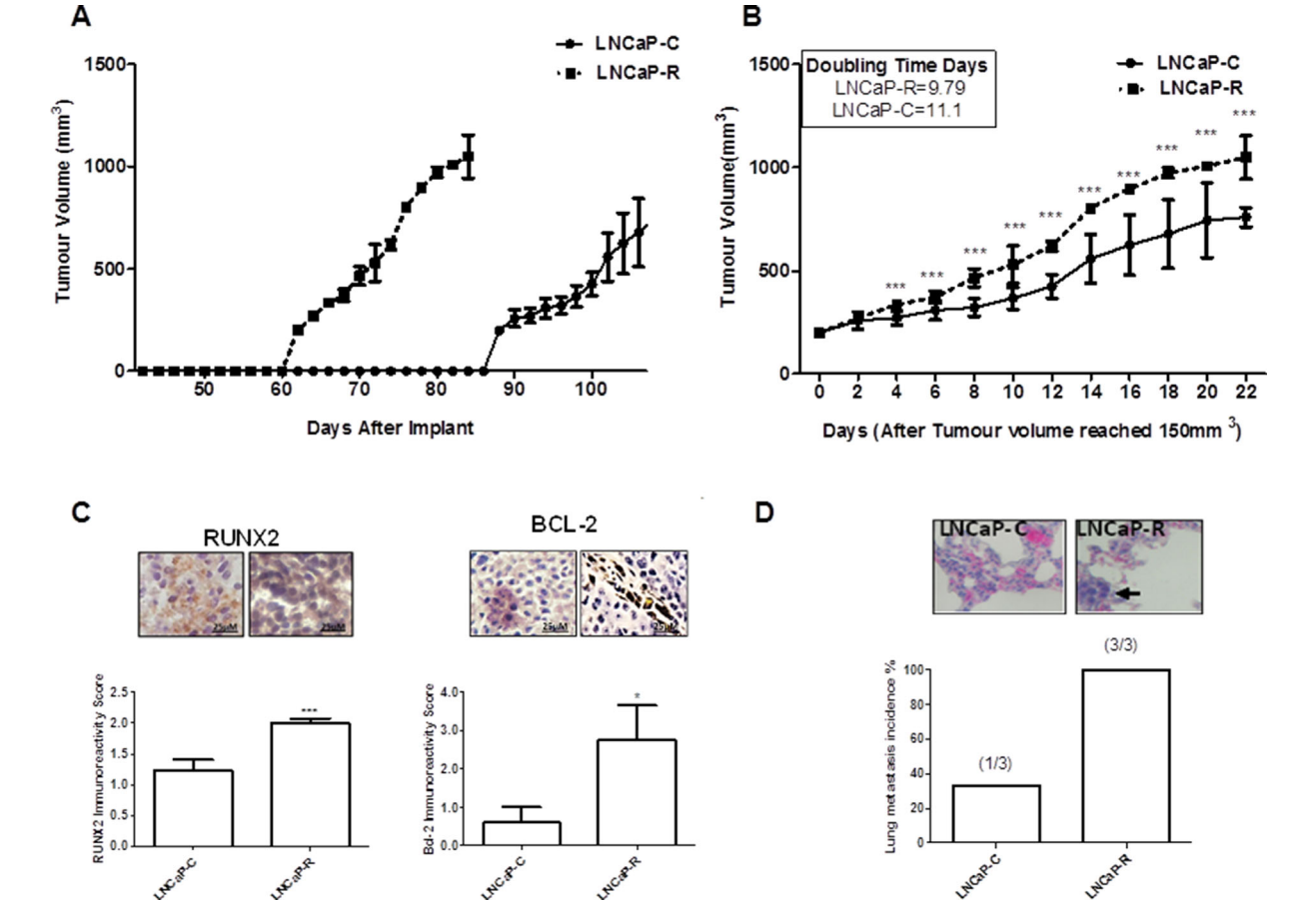

Fig. 5. Effect of RUNX2 over-expression in LNCaP tumours grown in vivo. LNCaP-C and LNCaP-R cells (1×10^6) were implanted on the rear dorsum of 6–8-week-old male SCID mice. (A) Tumour growth curve showing time taken after cell implantation to form a palpable tumour ($>150\,mm^3$). (B) Tumour growth curve showing difference in doubling time after palpable tumours form. Day 0 represents tumour size of $\sim 150\,mm^3$. (C) Tumours were excised from three mice at the experimental endpoint and processed for immunohistochemistry. Graph shows immunostaining score for RUNX2 and Bcl-2, with representative images inset (X200 magnification). (D) Lungs were excised from three mice at the experimental endpoint and processed for H & E staining. Lung metastasis incidence % was calculated. Three animals were allocated per group. Three animals were allocated per group. $^{*}P \leq 0.05$, $^{***}P \leq 0.001$ (Students *t*-test).

since inhibition of RUNX2 with targeted siRNA blocked Bcl-2 induction by NO (Fig. 4B and C). Further evidence of this was provided by a ChIP assay, which confirmed that RUNX2 displayed increased occupancy of the Bcl-2 promoter in the presence of NO. This agrees with our previous study that showed silencing RUNX2 caused a decrease in Bcl-2 expression due to the lack of RUNX2 binding to the Bcl-2 promoter (Browne et al., 2012). Having established these links, we investigated cell survival in the presence of docetaxel, a drug commonly used to treat advanced prostate cancer. We established that prostate cells treated with NO (10 μM) displayed increased cell viability following docetaxel treatment; however, in cells which had RUNX2 silenced by targeted siRNA, the effect was significantly abrogated (Fig. 4F). This suggests that NO confers protection against docetaxel, presumably by up-regulating RUNX2 and Bcl-2 levels, a protection which is lost if RUNX2 action is inhibited. The role of NO in the chemoresistance is complex, with various studies showing that that NO sensitises cancer cells to different drugs (Muir et al., 2006; Frederiksen et al., 2007), whilst others show that it confers resistance upon cancer cells (Fetz et al., 2009; Yu et al., 2013). Our study is the first to propose that NO is involved in induced chemoresistance in prostate cancer cells through the induction of RUNX2. This effect is likely to be further promoted by the impact of NO and/or RUNX2 on other downstream targets such as those involved in angiogenesis (VEGF) and inflammatory signalling (IL-8) and metastasis (MMP9 and MMP13) (Akech et al., 2010). Our observations also recall previous studies showing that NO induction in response to photostress confers a pro-survival effect through enhanced apoptotic resistance in breast and prostate cancer cells (Bhowmick and Girotti, 2013, 2014).

Given our findings above, we then investigated the effect of RUNX2 overexpression on tumour growth in vivo. When these LNCaP-R cells were grown as solid tumours in SCID mice the tumours became palpable on average 26 days earlier and had a faster doubling time compared to control tumours (Fig. 5A and B); this correlated with previous in vivo studies in breast and prostate mouse models of cancer. We also confirmed that the expected increase in RUNX2 and Bcl-2 occurred in the tumours grown in vivo (Fig. 5C). Furthermore, mice implanted with LNCaP-R tumour cells had more metastatic lung deposits than control mice, implicating RUNX2 over-expression in tumour spread (Fig. 5D), the involvement of

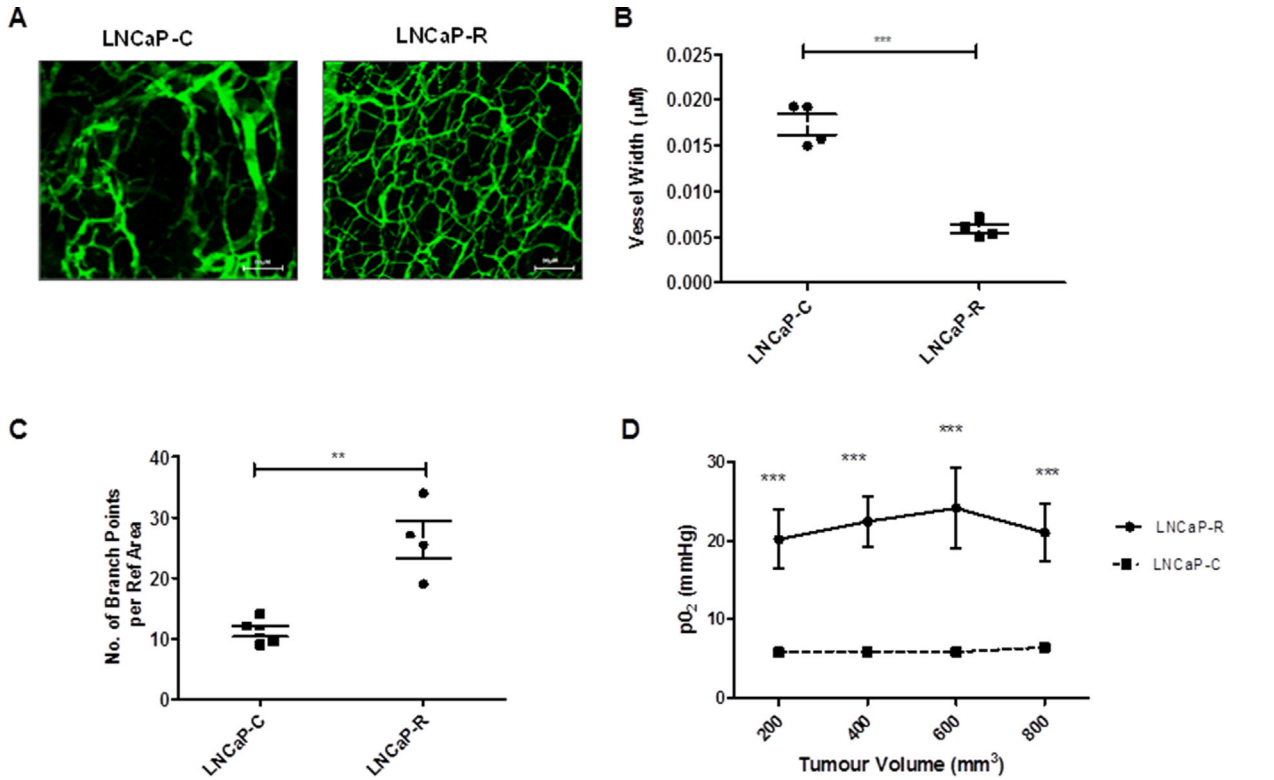

Fig. 6. Impact of RUNX2 elevation on tumour vascularisation. Window chambers were surgically implanted on the rear dorsum of male SCID mice with LNCaP-C or LNCaP-R cells embedded in matrigel and allowed to vascularise for 10 days. Representative images are shown in (A). (B and C) Quantified vessel width, number of branch points and vessel coverage (five images per mouse). (D) Oxylite electrode measurements of pO_2 in both tumour types during growth sizes (200–800 mm^3). 3 animals were allocated per group. $^{**}P \leq 0.01$, $^{***}P \leq 0.001$.

RUNX2 enhancing lung metastasis has been recently noted by Zhang et al. (2014). The anti-apoptotic effect caused by the RUNX2-mediated induction of Bcl-2 has been previously noted in osteoblasts (Ho et al., 2009), breast cancer cells (Pratap et al., 2009), renal tubuloepithelial cells (Ardura et al., 2013) and in chondrocytes of transgenic mice with elevated RUNX2 expression (Ding et al., 2012). Our study is consistent with these studies and is the first to report this relationship in an in vivo mouse model of prostate cancer.

The faster tumour growth characteristics of LNCaP-R tumours suggested that the tumour microenvironment might be modified. Therefore, we investigated the vasculature in these tumours using the dorsal skin flap model. LNCaP-R tumours showed a markedly normalised vasculature with a more even distribution of microvessels. Although the overall vessel coverage was approximately the same (data not shown) the LNCaP-R tumours had more vessels that were significantly smaller and with more branch points than observed in controls (Fig. 6A–C); these features allow better delivery of oxygen and nutrients than the more abnormal vasculature seen in the control tumours. The improved oxygenation of LNCaP-R tumours was confirmed in sub-cutaneous tumours (23 mmHg, 3.03% O_2), and is in distinct contrast to control LNCaP tumours, which we have shown to be considerably more hypoxic (5.85 mmHg, 0.77% O_2) (Ming et al., 2013). Both of these changes could make a significant contribution to tumour growth and they are consistent with the data presented in Figure 5. The influence of RUNX2 over-expression on angiogenesis in prostate tumours has not previously been reported. However, the data are consistent with a previous report that has implicated RUNX2 over-expression in the enhancement of angiogenesis in an in vitro model of hypertrophic chondrocytes (Lee et al., 2012).

Previously, it has been suggested that the normalisation of vessels during cancer therapy may aid in the control of tumour growth (Jain, 2005; Goel et al., 2011). However, our data show that vessel normalisation, mediated through RUNX2 over-expression, may be associated with improved oxygenation, faster tumour growth and enhanced Bcl2-expression. Although the improved vascular structure of LNCaP-R tumours could allow better drug delivery, the presence of increased Bcl-2 could reduce the apoptotic potential of the cancer cells being targeted by the therapy. Overall, our studies suggest that these changes facilitate tumour growth and progression to a more aggressive phenotype with a likely increase in treatment resistance related to the increase in Bcl-2.

In conclusion, we have shown that NO is capable of regulating RUNX2 expression in prostate cancer cells. At relatively low NO levels, RUNX2 expression was increased via several mechanisms including transcriptional control, transcript stability and relevant cancer-associated signalling pathways. The up-regulation of RUNX2 increased Bcl-2 both in vitro and in vivo; we had previously shown that this was associated with inhibition of apoptosis in these cells (Browne et al., 2012). When the RUNX2 over-expressing cells were grown in mice, the tumours developed enhanced growth characteristics therefore attributing to an improved tumour vasculature and increased oxygenation. Thus, silencing RUNX2

expression, either by manipulating NO levels or by direct targeting, may be a novel and attractive strategy for the treatment of prostate cancer.

Authors Contributions

HN carried out in vitro and in vivo work and drafted manuscript. GB created a stable RUNX2 over expressing cell line and was involved in drafting manuscript. KOD participated in molecular work, such as Q-PCR and western blotting. NB contributed to in vivo work, including tumour implantation and tumour measurements. JW participated in window chamber experiments. SMcK was involved in re-drafting paper. DMcK participated in paper design, figure layout and re-drafting manuscript.

Acknowledgment

We thank the Stein/Lian Laboratory (University of Vermont, USA) for kindly providing RUNX2 mutant constructs used in this study.

Literature Cited

Akech J, Wixted JJ, Bedard K, van der Deen M, Hussain S, Guise TA, van Wijnen AJ, Stein JL, Languino LR, Altieri DC, Pratap J, Keller E, Stein GS, Lian JB. 2010. Runx2 association with progression of prostate cancer in patients: Mechanisms mediating bone osteolysis and osteoblastic metastatic lesions. Oncogene 29:811–821.

Ardura JA, Sanz AB, Ortiz A, Esbrit P. 2013. Parathyroid hormone-related protein protects renal tubuloepithelial cells from apoptosis by activating transcription factor Runx2. Kidney Int 83:825–834.

Bakheet T, Williams BR, Khabar KS. 2003. ARED 2.0: An update of AU-rich element mRNA database. Nucleic Acids Res 31:421–423.

Bhowmick R, Girotti AW. 2013. Cytoprotective signaling associated with nitric oxide upregulation in tumor cells subjected to photodynamic therapy-like oxidative stress. Free Radic Biol Med 57:39–48.

Bhowmick R, Girotti AW. 2014. Pro-survival and pro-growth effects of stress-induced nitric oxide in a prostate cancer photodynamic therapy model. Cancer Lett 343:115–122.

Braconi C, Bracci R, Bearzi I, Bianchi F, Sabato S, Mandolesi A, Belvederesi L, Cascinu S, Valeri NN, Cellerino R, 2008. Insulin-like growth factor (IGF) 1 and 2 help to predict disease outcome in GIST patients. Ann Oncol 19:1293–1298.

Browne G, Nesbitt H, Ming L, Stein GS, Lian JB, McKeown SR, Worthington J. 2012. Bicalutamide-induced hypoxia potentiates RUNX2-mediated bcl-2 expression resulting in apoptosis resistance. Br J Cancer 107:1714–1721.

Brune B. 2003. Nitric oxide: NO apoptosis or turning it ON? Cell Death Differ 10:864–869.

Burke AJ, Sullivan FJ, Giles FJ, Glynn SA. 2013. The yin and yang of nitric oxide in cancer progression. Carcinogenesis 34:503–512.

Butterworth KT, McCarthy HO, Devlin A, Ming L, Robson T, McKeown SR, Worthington J. 2008. Hypoxia selects for androgen independent LNCaP cells with a more malignant geno- and phenotype. Int J Cancer 123:760–768.

Cronauer MV, Ince Y, Engers R, Rinnab L, Weidemann W, Suschek CV, Burchardt M, Kleinert H, Wiedenmann J, Sies H, Ackermann R, Kröncke KD. 2007. Nitric oxide-mediated inhibition of androgen receptor activity: Possible implications for prostate cancer progression. Oncogene 26:1875–1884.

Damoulis PD, Drakos DE, Gagari E, Kaplan DL. 2007. Osteogenic differentiation of human mesenchymal bone marrow cells in silk scaffolds is regulated by nitric oxide. Ann NY Acad Sci 11:367–376.

Ding M, Lu Y, Abbassi S, Li F, Li X, Song Y, Geoffroy V, Im HJ, Zheng Q. 2012. Targeting Runx2 expression in hypertrophic chondrocytes impairs endochondral ossification during early skeletal development. J Cell Physiol 227:3446–3456.

Drissi H, Luc Q, Shakoori R, Chuva De Sousa Lopes S, Choi JY, Terry A, Hu M, Jones S, Neil JC, Lian JB, Stein JL, Van Wijnen AJ, Stein GS. 2000. Transcriptional autoregulation of the bone related CBFA1/RUNX2 gene. J Cell Physiol 184:341–350.

Fetz V, Bier C, Habtemichael N, Schuon R, Schweitzer A, Kunkel M, Engels K, Kovács AF, Schneider S, Mann W, Stauber RH, Knauer SK. 2009. Inducible NO synthase confers chemoresistance in head and neck cancer by modulating survivin. Int J Cancer 124:2033–2041.

Frederiksen LJ, Sullivan R, Maxwell LR, Macdonald-Goodfellow SK, Adams MA, Bennett BM, Siemens DR, Graham CH. 2007. Chemosensitization of cancer in vitro and in vivo by nitric oxide signaling. Clin Cancer Res 13:2199–2206.

Fujita T, Fukuyama R, Enomoto H, Komori T. 2004. Dexamethasone inhibits insulin-induced chondrogenesis of ATDC5 cells by preventing PI3K-akt signaling and DNA binding of Runx2. J Cell Biochem 93:374–383.

Ge C, Xiao G, Jiang D, Franceschi RT. 2007. Critical role of the extracellular signal-regulated kinase-MAPK pathway in osteoblast differentiation and skeletal development. J Cell Biol 176:709–718.

Goel S, Duda DG, Xu L, Munn LL, Boucher Y, Fukumura D, Jain RK. 2011. Normalization of the vasculature for treatment of cancer and other diseases. Physiol Rev 91:1071–1121.

Haby C, Aunis D, Zwiller J. 1994. Okadaic acid induces activator protein 1 activity and immediate early gene transcription in rat pheochromocytoma cells. mechanism of action. Biochem Pharmacol 48:819–825.

Ho WP, Chan WP, Hsieh MS, Chen RM. 2009. Runx2-mediated bcl-2 gene expression contributes to nitric oxide protection against hydrogen peroxide-induced osteoblast apoptosis. J Cell Biochem 108:1084–1093.

Jain RK. 2005. Antiangiogenic therapy for cancer: Current and emerging concepts. Oncology 19:7–16.

Jibiki I, Hashimoto S, Maruoka S, Gon Y, Matsuzawa A, Nishitoh H, Ichijo H, Horie T. 2003. Apoptosis signal-regulating kinase 1-mediated signaling pathway regulates nitric oxide-induced activator protein-1 activation in human bronchial epithelial cells. Am J Respir Crit Care Med 167:856–861.

Komori T. 2003. Requisite roles of Runx2 and cbfb in skeletal development. J Bone Miner Metab 21:193–197.

Lee SH, Che X, Jeong JH, Choi JY, Lee YJ, Lee YH, Bae SC, Lee YM. 2012. Runx2 protein stabilizes hypoxia-inducible factor-1alpha through competition with von hippel-lindau protein (pVHL) and stimulates angiogenesis in growth plate hypertrophic chondrocytes. J Biol Chem 287:14760–14771.

Mayor S. 2012. Latest UK figures show increase in prostate cancer diagnoses and falling death rate. BMJ 344:e3252.

Ming L, Byrne NM, Camac SN, Mitchell CA, Ward C, Waugh DJ, Mc Keown SR, Worthington J. 2013. Androgen deprivation results in time-dependent hypoxia in LNCaP prostate tumours: Informed scheduling of the bioreductive drug AQ4N improves treatment response. Int J Cancer 132:1323–1332.

Muir CP, Adams MA, Graham CH. 2006. Nitric oxide attenuates resistance to doxorubicin in three-dimensional aggregates of human breast carcinoma cells. Breast Cancer Res Treat 96:169–176.

Nanni S, Benvenuti V, Grasselli A, Priolo C, Aiello A, Mattiussi S, Colussi C, Lirangi V, Illi B, D'Eletto M, Cianciulli AM, Gallucci M, De Carli P, Sentinelli S, Mottolese M, Carlini P, Strigari L, Finn S, Mueller E, Arcangeli G, Gaetano C, Capogrossi MC, Donnorso RP, Bacchetti S, Sacchi A, Pontecorvi A, Loda M Farsetti. 2009. Endothelial NOS, estrogen receptor beta, and HIFs cooperate in the activation of a prognostic transcriptional pattern in aggressive human prostate cancer. J Clin Invest 119:1093–1108.

Pfeilschifter J, Eberhardt W, Huwiler A. 2001. Nitric oxide and mechanisms of redox signalling: Matrix and matrix-metabolizing enzymes as prime nitric oxide targets. Eur J Pharmacol 429:279–286.

Pratap J, Imbalzano KM, Underwood JM, Cohet N, Gokul K, Akech J, van Wijnen AJ, Stein JL, Imbalzano AN, Nickerson JA, Lian JB, Stein GS. 2009. Ectopic runx2 expression in mammary epithelial cells disrupts formation of normal acini structure: Implications for breast cancer progression. Cancer Res 69:6807–6814.

Pratap J, Wixted JJ, Gaur T, Zaidi SK, Dobson J, Veeraraj KD, Hussain S, van Wijnen AJ, Stein JL, Stein GS, Lian JB. 2008. Runx2 transcriptional activation of indian hedgehog and a downstream bone metastatic pathway in breast cancer cells. Cancer Res 68:7795–7802.

Rutberg SE, Adams TL, Olive M, Alexander N, Vinson C, Yuspa SH. 1999. CRE DNA binding proteins bind to the AP-1 target sequence and suppress AP-1 transcriptional activity in mouse keratinocytes. Oncogene 18:1569–1579.

Sheu SY, Tsai CC, Sun JS, Chen MH, Liu MH, Sun MG. 2012. Stimulatory effect of puerarin on bone formation through co-activation of nitric oxide and bone morphogenetic protein-2/mitogen-activated protein kinases pathways in mice. Chin Med J 125:3646–3653.

Shore P. 2005. A role for Runx2 in normal mammary gland and breast cancer bone metastasis. J Cell Biochem 96:484–489.

Sparkman L, Boggaram V. 2004. Nitric oxide increases IL-8 gene transcription and mRNA stability to enhance IL-8 gene expression in lung epithelial cells. Am J Physiol Lung Cell Mol Physiol 287:L764–L773.

Tabuchi A, Oh E, Taoka A, Sakurai H, Tsuchiya T, Tsuda M. 1996. Rapid attenuation of AP-1 transcriptional factors associated with nitric oxide (NO)-mediated neuronal cell death. J Biol Chem 271:31061–31067.

Wagner EF. 2002. Functions of AP1 (Fos/Jun) in bone development. Ann Rheum Dis 61:40–42.

Wai PY, Mi Z, Gao C, Guo H, Marroquin C, Kuo PC. 2006. Ets-1 and runx2 regulate transcription of a metastatic gene, osteopontin, in murine colorectal cancer cells. J Biol Chem 281:18973–18982.

Wang S, Zhang J, Zhang Y, Kern S, Danner RL. 2008. Nitric oxide-p38 MAPK signaling stabilizes mRNA through AU-rich element-dependent and -independent mechanisms. J Leukoc Biol 83:982–990.

Webb BA, Chimenti M, Jacobson MP, Barber DL. 2011. Dysregulated pH: A perfect storm for cancer progression. Nat Rev Cancer 11:671–677.

Workman P, Aboagye EO, Balkwill F, Balmain A, Bruder G, Chaplin DJ, Double JA, Everitt J, Farningham DA, Glennie MJ, Kelland LR, Robinson V, Stratford IJ, Tozer GM, Watson S, Wedge SR, Eccles SA; Committee of the National Cancer Research Institute. 2010. Guidelines for the welfare and use of animals in cancer research. Br J Cancer 102:1555–1577.

Xiao G, Jiang D, Gopalakrishnan R, Franceschi RT. 2002. Fibroblast growth factor 2 induction of the osteocalcin gene requires MAPK activity and phosphorylation of the osteoblast transcription factor, Cbfa1/Runx2. J Biol Chem 277:36181–36187.

Yu S, Jia L, Zhang Y, Wu D, Xu Z, Ng CF, To KK, Huang Y, Chan FL. 2013. Increased expression of activated endothelial nitric oxide synthase contributes to antiandrogen resistance in prostate cancer cells by suppressing androgen receptor transactivation. Cancer Lett 328:83–94.

Zhang X, Akech J, Browne G, Russell S, Wixted JJ, Stein JL, Stein GS, Lian JB. 2014. Runx2-Smad signalling impacts the progression of tumour-induced bone disease. Int J Cancer 136:1321–1332.

Supporting Information

Additional supporting information may be found in the online version of this article at the publisher's web-site.